Unbiased Analysis of the Impact of Micropatterned Biomaterials on Macrophage Behaviour Provides Insights beyond Pre-defined Polarisation States

*Sonali Singh [1], Dennis Awuah [1], Hassan M. Rostam [1, ‡], Richard D. Emes [2,3], Navrohit K. Kandola [1], David Onion [1], Su Su Htwe [1], Buddharaksa Rajchagool [1], Byung-Hyun Cha [4], Duckjin Kim [4], Patrick J. Tighe [1], Nihal E. Vrana [5,6], Ali Khademhosseini [4,7], Amir Ghaemmaghami [1]**

[1] Division of Immunology, School of Life Sciences, University of Nottingham, University Park, Nottingham, UK

[2] School of Veterinary Medicine and Science, University of Nottingham, Sutton Bonington Campus, Leicestershire, United Kingdom

[3] Advanced Data Analysis Centre, University of Nottingham, Sutton Bonington Campus, Leicestershire, United Kingdom

[4] Center for Biomedical Engineering, Department of Medicine, Brigham and Women's Hospital Harvard Medical School, Harvard-MIT Division of Health Sciences and Technology Massachusetts Institute of Technology, Cambridge, MA 02139, USA

[5] INSERM UMR 1121, 11 rue Humann, 67085 Strasbourg, France

[6] Protip Medical, 8 Place de l'Hôpital, 67000 Strasbourg, France

[7] Wyss Institute for Biologically Inspired Engineering at Harvard University, Boston, MA 02115, USA

* Corresponding author: email: amir.ghaemmaghami@nottingham.ac.uk, phone: +44 (0)115 82 30730

‡ Current address: Department of Biology, University of Garmian, Kurdistan

ABSTRACT: Macrophages are master regulators of immune responses towards implanted biomaterials. The activation state adopted by macrophages in response to biomaterials determines their own phenotype and function as well as those of other resident and infiltrating immune and non-immune cells in the area. A wide spectrum of macrophage activation states exists, with M1 (pro-inflammatory) and M2 (anti-inflammatory) representing either ends of the spectrum. In biomaterials research, cell-instructive surfaces that favour or induce M2 macrophages have been considered as beneficial due to the anti-inflammatory and pro-regenerative properties of these cells. In this study, we used a gelatin methacryloyl (GelMA) hydrogel platform to determine whether micropatterned surfaces can modulate the phenotype and function of human macrophages. The effect of microgrooves/ridges and micropillars on macrophage phenotype, function, and gene expression profile were assessed using conventional methods (morphology, cytokine profile, surface marker expression, phagocytosis) and gene microarrays. Our results demonstrated that micropatterns did induce distinct gene expression profiles in human macrophages cultured on microgrooves/ridges and micropillars. Significant changes were observed in genes related to primary metabolic processes such as transcription, translation, protein trafficking, DNA repair and cell survival. However, interestingly conventional phenotyping methods, relying on surface marker expression and cytokine profile, were not able to distinguish between the different conditions, and indicated no clear shift in cell activation towards an M1 or M2 phenotypes. This highlights the limitations of studying the effect of different physicochemical conditions on macrophages by solely relying on conventional markers that are primarily developed to differentiate between cytokine polarised M1 and M2 macrophages. We therefore, propose the adoption of unbiased screening methods in determining macrophage responses to biomaterials. Our data clearly shows that the exclusive use of conventional markers and methods for determining macrophage activation status could lead to missed opportunities for understanding and exploiting macrophage responses to biomaterials.

KEYWORDS: hydrogels, macrophages, immune modulation, gelatin methacryloyl, transcriptomics, micropatterns

INTRODUCTION

Macrophages are innate immune cells that play many roles in the body, including maintenance of tissue homeostasis, clearance of aging and damaged cells, phagocytosis and killing of microorganisms and the induction and regulation of inflammation and tissue repair[1]. They are able to perform these diverse functions due to their extreme plasticity. Macrophages have been shown to adopt a spectrum of activation states depending upon the prevailing microenvironment[2].

Of these multiple activation states, M1 (pro-inflammatory) and M2 (pro-wound healing) phenotypes, have been best characterised and are often used as reference points when describing intermediate macrophage phenotypes. Although the M1-M2 macrophage activation paradigm is a simplification of possible polarisation states, it can still be useful in determining whether macrophages lie towards the pro-inflammatory end or the anti-inflammatory/pro-wound healing end of the activation spectrum[3]. In order to distinguish the activation state, macrophages are commonly characterised on the basis of properties such as the expression of cellular markers, cytokine profile and phagocytic ability[4].

M1 macrophages secrete pro-inflammatory cytokines such as interleukin 12 (IL-12), IL-23, tumour necrosis factor alpha (TNF-α), IL-6, and IL-1β[5-7]. They also demonstrate elevated expression of the chemokine (C-C motif) receptor 2 (CCR2), CCR7, calprotectin, and inducible nitric oxide synthase 2 (iNOS2)[8-11]. By comparison, M2 macrophages produce high levels of anti-inflammatory and pro-fibrotic cytokines such as IL-1 receptor antagonist (IL-1RA), IL-10, transforming growth factor (TGF-β), and CCL18[7, 12-13]. Additionally, these cells are characterised by high expression of the mannose receptor (MR, CD206) and the scavenger receptor CD163[8, 11-12, 14].

An environmental determinant of macrophage phenotype that has long been recognised is the substrate on which macrophages grow. It has been demonstrated that cells, including macrophages, respond to the biological, chemical, physical and mechanical properties of a substrate. The increasing use of natural and synthetic materials for biomedical applications such as drug delivery, implants, stents, pacemakers and catheters have accelerated research into the immune response, and more particularly the macrophage

response to substrates[15], and how different physicochemical properties of a given material could affect macrophage phenotype and function [16-17].

One class of materials that is gaining popularity both in biomedical research and tissue engineering are hydrogels. Hydrogels are composed of a cross-linked network of hydrophilic polymers capable of absorbing water and swelling to many times their original size[18]. These gels may be natural or synthetic in origin and have a wide range of physical, chemical and biological properties[18]. In addition, hydrogels can be relatively easily modified to achieve desired topographies, stiffness and biofunctional characteristics (e.g. arginine-glycine-aspartic acid (RGD) sites for cell attachment)[19].

Research into the response to hydrogels has tended to focus on *in vivo* responses in mice and non-human primates[20-22]. Only a few studies have looked specifically at the response of macrophages to hydrogels[23]. Gelatin methacryloyl (GelMA) hydrogels are becoming increasingly popular as they combine the bioactivity of gelatin with the tunability of a photo-crosslinkable hydrogel[19, 24]. Since GelMA is synthesised from gelatin, which is a hydrolysis product of collagen (one of the major extracellular matrix (ECM) proteins), it is biocompatible and does not elicit a strong immune response[24]. In addition, it has RGD motifs and matrix metalloproteinase (MMP) target sites, which aid cell adhesion and matrix remodelling, respectively[25-26]. GelMA has been used in applications such as regenerative medicine, drug delivery, biosensing, cell signalling, and *in vitro* 3D cell culture[24].

The aim of this study was to characterise human macrophage responses to microtopographies on GelMA hydrogel. Substrate topography affects factors such as cell attachment, cytoskeleton organisation, and cell and nuclear shape and orientation[27-30]. Other groups have investigated the effect of substrate topography on mouse macrophages and human monocyte/macrophage cell lines using a variety of materials such as polyethylene films, Polydimethylsiloxane (PDMS), electrospun scaffolds, expanded polytetrafluoroethylene (PTFE) and titanium[31-35]. Paul *et al.* compared the response of human primary monocyte-derived macrophages to microstructured and nanotextured polyvinylidene fluoride (PVDF)

surfaces[36]. However, there is little information on the effect of different micropatterned hydrogels on the phenotype and function of human primary macrophages.

Thus, in this study we first used soft photolithography to fabricate micropattenred GelMA hydrogels followed by investigating the response of human monocyte-derived macrophages to such different microtopographies. We mainly focused on two topographies namely micropillars (height=20 μm, diameter=20 μm, distance between pillars=5 μm) and microgrooves/ridges (depth=20 μm, groove width=20 μm, ridge width=10 μm) to determine the effect of focal point adhesion (micropillars) and cell elongation (microgrooves/ridges) on macrophage phenotype and function using conventional markers (i.e. macrophage morphology, surface marker expression, cytokine profile and phagocytosis) as well as their gene expression profile covering the whole genome.

MATERIALS AND METHODS

Materials

All materials were purchased from Sigma-Aldrich unless otherwise stated.

Micropatterned hydrogel fabrication

Coating glass slides with 3-(Trimethoxysilyl)propyl methacrylate (TMSPMA)

TMSPMA coating was carried out as previously described[37] with some modifications. Briefly, glass slides were submerged in 10% (*w/v*) NaOH overnight at room temperature, washed first with distilled water then 100% ethanol, and air-dried. Slides were then baked at 80ºC for 1 h, coated with TMSPMA and baked at 80ºC overnight. TMSPMA-coated slides were washed with 100% ethanol, dried, and baked for 1-2 h at 80ºC.

Coating TMSPMA glass slides with poly(2-hydroxyethyl) methacrylate (polyHEMA)

Coating TMSPMA-treated slides with polyHEMA was performed as previously described[38] with some modifications. Briefly, TMSPMA glass slides were cleaned with 100% ethanol, air-dried, dipped in 4.5%

(*w/v*) polyHEMA in ethanol 2-3 times, and air-dried for 3 days.

Fabrication of micropatterned GelMA hydrogels

Hydrogel preparation and fabrication were performed by a two-step photolithography process as previously described[39-40] with some modifications. 15% (*w/v*) GelMA solution in 0.5% (*w/v*) photoinitiator (2-hydroxy-4'-(2-hydroxyethoxy)-2-methylpropioprenone) in PBS was prepared at 60ºC in the dark. A drop of GelMA was placed on a TMSPMA-polyHEMA coated glass slide, and a polydimethylsiloxane (PDMS) mould with the required pattern was placed on top of the gel. GelMA was then photocrosslinked with UV (Omnicure 2000) at 800 mW for 9.5 s with 8 cm distance between UV source and the sample. The micropatterns used were: 1) microgrooves: depth=20 µm, ridge width=10 µm, groove distance=20 µm, and 2) micropillars: depth=20 µm, pillar diameter=20 µm, distance between pillars=5 µm. Unpatterned hydrogels were also fabricated as controls.

The hydrogels were UV sterilised for 30 min, transferred to 24-well non-tissue culture (TC)-treated plates (Corning Life Sciences), and incubated in antibiotic-antimycotic (Ab/Am) solution (500 U/ml penicillin, 0.5 mg/ml streptomycin and 1.25 µg/ml amphotericin B in citrate buffer) overnight at 37ºC, 5% CO_2 in a humidified incubator. Hydrogels were washed once with complete RPMI medium (RPMI-1640 medium supplemented with 10% (*v/v*) foetal bovine serum (FBS), 2 mM L-glutamine, 100 U/ml penicillin, and 100 µg/ml streptomycin) to remove the residual photoinitiator before cells were seeded.

Monocyte-derived macrophage generation

Buffy coats were obtained from the National Blood Service (Sheffield, UK) following Ethics committee approval. Peripheral blood mononuclear cells (PBMCs) were obtained from heparinised blood by Histopaque-1077 density gradient centrifugation. Monocytes were isolated from PBMCs using the MACS magnetic cell separation system (positive selection with CD14 MicroBeads and LS columns, Miltenyi Biotec) as described before[41].

Purified monocytes were suspended in complete RPMI medium containing 50 ng/ml M-CSF (Miltenyi Biotec) and seeded at $1x10^6$ cells/well in 24-well ultra-low attachment plates (Corning Life Sciences).

The cells were incubated at 37°C, 5% CO_2 in a humidified incubator for 6 days, with fresh medium and cytokines added on Day 3.

Macrophage culture on GelMA hydrogels

Monocyte-derived macrophages were harvested from the ultra-low attachment plates by placing the plates on ice for 20 min followed by gentle pipetting to collect detached cells. The macrophages were then washed, resuspended in fresh complete RPMI medium containing 50 ng/ml M-CSF, and $2.5x10^5$ macrophages were seeded per patterned hydrogel ($\approx 1.32x10^5$ macrophages/cm^2) inside 24-well non-Tissue Culture (TC)-treated plates. For tissue culture-treated plastic (TCP) controls, $2.5x10^5$ macrophages prepared as described above were also seeded per well of a 24-well TC-treated plate. After overnight incubation at 37°C, 5% CO_2 in a humidified incubator, the cell-laden hydrogels were transferred to new non-TC plates containing fresh complete RPMI medium and 50 ng/ml M-CSF and incubated again. For TCP controls, the medium was changed at the same time. Macrophages were cultured on the GelMA hydrogels and TCP controls for a total of 3 days. For lipopolysaccharide (LPS)-stimulated samples, macrophages cultured on TCP or hydrogels for 3 days were then treated with 200 ng/ml LPS at 37°C, 5% CO_2 for 24 h.

Morphological analysis of macrophages

Cells were fixed with 4% paraformaldehyde (PFA) in PBS, washed twice with PBS (5 min per wash), then permeabilised with 0.2 % Triton-X100 in PBS for 20 min. All the steps in this procedure were carried out at room temperature. After 2 further washes with PBS, non-specific binding was blocked with 5% goat serum in PBS as described in the previous section. This was followed by 2 washes with PBS and cytoskeleton staining of F-actin with 5 µg/ml Alexa Fluor® 488 Phalloidin (Cell Signalling Technology) in 1% goat serum and 0.1% sodium azide for 30 min. Cells were then washed 3 times with PBS and stained with 250 ng/ml DAPI (4',6-Diamidino-2-Phenylindole) (Invitrogen) in PBS for 5 min, washed 3 times with PBS, then mounted on a slide with Fluoromount™ mounting medium. Samples

were then imaged using an IMSTAR automated fluorescent microscope (IMSTAR S.A., France), which took ~100 images per sample.

Images were loaded into CellProfiler software (Broad Institute, Harvard, USA)[42] and metadata detailing the cell type in the image was extracted from the file name. Primary detection of the cell nucleus (DAPI channel), followed by secondary detection of the cell body (F-actin channel) were optimised following which the full dataset of images was analysed by the software and a database containing a range of cell descriptors such as perimeter, area, major and minor axes, etc. was generated. For each sample, the means of these descriptors were calculated and used for generating graphs and conducting statistical analyses.

Flow cytometric analysis of mannose receptor (MR) and calprotectin

Macrophages were detached from the hydrogels or TCP by using 1 mg/ml collagenase A (Roche) in PBS or non-enzymatic cell dissociation buffer, respectively, and placing on ice for 40 min, then washed once with PBA (0.5% (*w/v*) bovine serum albumin (BSA) and 0.1% (*w/v*) sodium azide in PBS). Cells were blocked with 5% (*v/v*) human serum in PBS at 4ºC for 60 min, then washed once with PBA. 2 µg/ml mouse anti-human anti-calprotectin antibody (Thermo Scientific Pierce) and 8 µg/ml PE/Cy5-labelled mouse anti-human anti-CD206 antibody (for labelling the mannose receptor, MR) (BioLegend) were added and samples incubated at 4ºC for 30 min. After one wash with PBA, 4 µg/ml of Alexa Fluor 647-labelled rabbit anti-mouse IgG (H+L) secondary antibody (Invitrogen) was added to the tubes containing the anti-calprotectin primary antibody and samples were incubated at 4ºC for 30 min. The samples were washed a final time with PBA and fixed with 0.5% (*v/v*) PFA in PBS. Samples were run on an FC500 flow cytometer (Beckman Coulter) and the analysis was carried out using Weasel software (Walter and Eliza Hall Institute of Medical Research).

Cytokine quantification

Supernatants were collected and assayed for the cytokines TNF-α, IL-12, IL-1β, CCL18, and IL-1RA by ELISA as per the manufacturer's instructions (Table 1).

Table 1. ELISA kits used in this study

Cytokine	ELISA Kit supplier
IL-1β	Antibody Solutions AS56-P, AS57-B (Capture and detection antibodies) Peprotech 200-01B (Standard protein)
IL-1RA	PeproTech 900-K474
IL-12	PeproTech 900-K96
CCL18	R&D Systems DY394
TNFα	Peprotech 900-K25

Phagocytosis

Macrophages were treated with 10 particles/cell of Alexa Fluor 488-labelled zymosan (Molecular Probes) in complete RPMI medium at 37ºC, 5% CO_2 for 30 min. Cells were then washed 3 times with PBS and fixed with 4% PFA in PBS for 10 min. Cells were washed again 3 times with PBS and detached from the gels or TCP as described in the section above (Flow cytometric analysis of MR and calprotectin). Cells were then harvested, washed once with PBA and resuspended in PBA prior to running on a MoFlo Astrios EQ flow cytometer (Beckman Coulter). Analysis was carried out using Kaluza Analysis 1.5 software (Beckman Coulter).

Mean number of particles per zymosan-positive cell was calculated using the formula: (Median fluorescence intensity (MFI) of zymosan-positive cells – MFI of untreated cells)/MFI of zymosan particles. Phagocytic index was calculated as: percentage of zymosan-positive cells x mean number of particles per positive cell.

mRNA preparation

Samples were washed twice with cold PBS. Total RNA was isolated with Trizol reagent using the PureLink® RNA mini kit, (Ambion, Thermo Fisher Scientific). RNA quality was assessed on an Agilent 2100 Bioanalyzer (Agilent Technologies) and samples with RNA integrity (RIN) values ≥ 7 were used

for microarray analyses.

Gene Microarrays

Preparation of cRNA, hybridization and scanning of Agilent arrays was done using the One Colour Microarray-based Gene Expression Analysis (Agilent Technologies) according to manufacturer's protocol. Briefly, 200 ng of total RNA was labelled with T7-linked oligo-dT primers for first-strand cDNA synthesis. Subsequently, labelled cRNA was generated from cDNA using T7 RNA polymerase with cyanine 3-CTP dye. The labelled cRNA was then purified using the RNeasy mini kit (Qiagen) and quantified using a NanoDrop ND1000 spectrophotometer (Thermo Scientific). For each sample, 1.65 µg cRNA was fragmented at 60°C for 30 min in fragmentation buffer, following which the 2x Hi-RPM Hybridization Buffer was used to stop the fragmentation reaction. Samples were centrifuged at 13,000 rpm for 1 min and immediately hybridized to Agilent oligo microarrays in a hybridization chamber. The assembled chamber was placed in a rotator oven (set at 10 rpm) and incubated at 65°C for 17 h. Slides were washed in pre-warmed gene expression wash buffers containing 0.005% (*v/v*) Triton X-102 (10%) and scanned with the GenePix® 4200 AL Microarray Scanner (Axon, Molecular devices, CA).

Gene Microarray analysis

Preliminary filtering and normalisation of data were carried out in JExpress Pro 2012 software. For each donor, data on gels were quantile normalised to their respective TCP controls to obtain relative expression values. Using R software, data from each individual array probe were processed. An ANOVA and a pairwise Tukey's post hoc test were conducted to identify conditions causing significant changes in gene expression. Principal component analysis and heatmaps of relative expression for all significant genes $p<0.01$ and $p<0.05$ were also generated for the R analysis.

Statistical analysis

A minimum of 3 donors (3 independent replicates) were tested for each assay. Graphs depict mean data from each donor as individual symbols in addition to the mean ± standard deviation (SD) of all donors used, while microscope images and histograms are from a representative donor. Statistical

analyses were performed in GraphPad Prism v 6.05. Significance was calculated by one-way ANOVA with Tukey's post hoc test, $p \leq 0.05$ was considered significant.

RESULTS

In order to determine the effect of GelMA micropatterning on human primary macrophages, the first step was to select GelMA hydrogels of appropriate rigidity to permit high fidelity micropatterning and good cell attachment. Three distinct stiffness of GelMA were selected – 5%, 10%, and 15% GelMA with compressive moduli of 2.96 ± 0.28 kPa, 16.66 ± 0.95 kPa, and 25.82 ± 1.50 kPa, respectively (Figure S1A in Supporting Information). 15% (*w/v*) GelMA was found to be the most appropriate for further use as it could be micropatterned with high fidelity and allowed macrophage attachment and interaction with the hydrogel surface (Figures S1 and S2 in Supporting Information).

Macrophage morphology on GelMA hydrogels

Macrophages cultured on micropatterned GelMA hydrogels and tissue culture-treated plastic (TCP) both exhibited heterogeneous morphologies (Figure 1A). Depending upon the hydrogel patterning employed, cell alignment was also altered, e.g. alignment in one direction on microgrooves/ridges compared with random attachment on micropillars and unpatterned hydrogels (Figure 1A).

However, analysis of macrophages cultured on these different surfaces using CellProfiler software[42] revealed that alterations in cell morphology were insignificant amongst hydrogel conditions. Instead, it appeared that macrophages cultured on GelMA hydrogels (regardless of topographies) were significantly smaller and had a significantly lower cytoplasm to nucleus ratio than those cultured on TCP (Figure 1B). Cells on GelMA were also significantly more elongated than those on TCP, as measured by the cell major to minor axis ratios (Figure 1B).

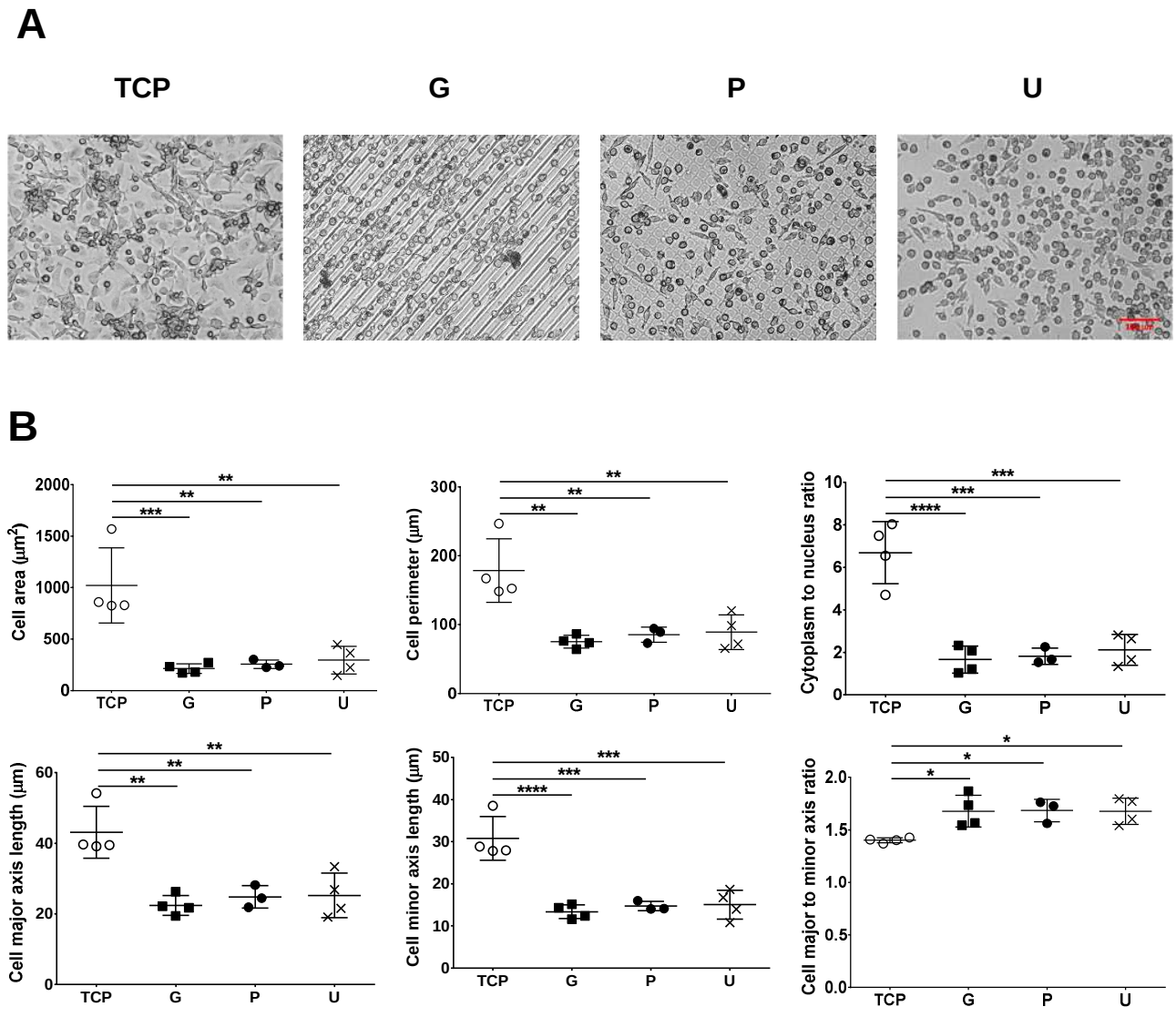

Figure 1. Morphology of human monocyte-derived macrophages on GelMA hydrogel micropatterns. Human monocyte-derived macrophages were cultured on TCP (tissue culture plastic controls) and GelMA micropatterns: G, microgrooves/ridges; P, micropillars; U, unpatterned for 3 days. **A.** Representative phase contrast images. Scale bar=100 µm. **B.** CellProfiler analysis of macrophage dimensions (µm or µm^2) on the different surfaces. Data presented are mean ± SD for at least n=3 donors. Significance was calculated by a one-way ANOVA with Tukey's post hoc test, * $p \leq 0.05$, ** $p \leq 0.01$, *** $p \leq 0.001$.

Phenotyping macrophages on patterned GelMA hydrogels by conventional means

Next, it was tested whether culturing macrophages on micropatterned GelMA hydrogels altered conventional indicators of macrophage activation such as surface marker expression, cytokine profile, and phagocytic activity.

No significant differences were observed in the percentage of positive cells or the expression (median fluorescence intensity) of MR or calprotectin (used here as M2 and M1 markers respectively) under any of the conditions (Figure S3 in Supporting Information).

Three pro-inflammatory (TNF-α, IL-12, IL-1β) and two anti-inflammatory (IL-1RA, CCL18) cytokines were quantified in the supernatants of unstimulated macrophages and LPS-stimulated macrophages. Since less cells were present in the GelMA conditions than in TCP due to the smaller size of the GelMA patterns, cytokine values for the different conditions were normalised for cell number. The cytokine data presented here are cytokine concentration in pg/ml per 10^4 cells (Figure 2).

No significant differences were observed between TNF-α, IL-12, IL-1RA, and CCL18 production by macrophages on the different GelMA topographies (Figure 2), possibly due to the small sample size, however some trends were observed. For example IL-1RA production by cells on microgrooves/ridges and unpatterned GelMA tended to be higher than levels produced by cells on micropillars (or TCP) both pre- and post-LPS stimulation (Figure 2). Furthermore, in LPS-stimulated macrophages, CCL18 production appeared to be increased on unpatterned GelMA compared to microgrooves/ridges or micropillars (Figure 2).

Whilst no significant differences were observed between unstimulated macrophages cultured on TCP vs. GelMA, upon LPS stimulation of these cells, it was observed that microgroove/ridge and micropillar patterning on GelMA significantly reduced the production of TNF-α compared to unpatterned GelMA ($p=0.0196$), bringing TNF-α production in line with that observed on TCP (Figure 2). Macrophages on unpatterned GelMA were also found to produce significantly more IL-1RA than those on TCP following LPS stimulation ($p=0.0250$, Figure 2). No significant differences were observed in the production of IL-

12 or CCL18 between any of the conditions (Figure 2). IL-1β production was also measured in these samples, but was found to be negligible in all conditions pre- and post-LPS stimulation (data not shown).

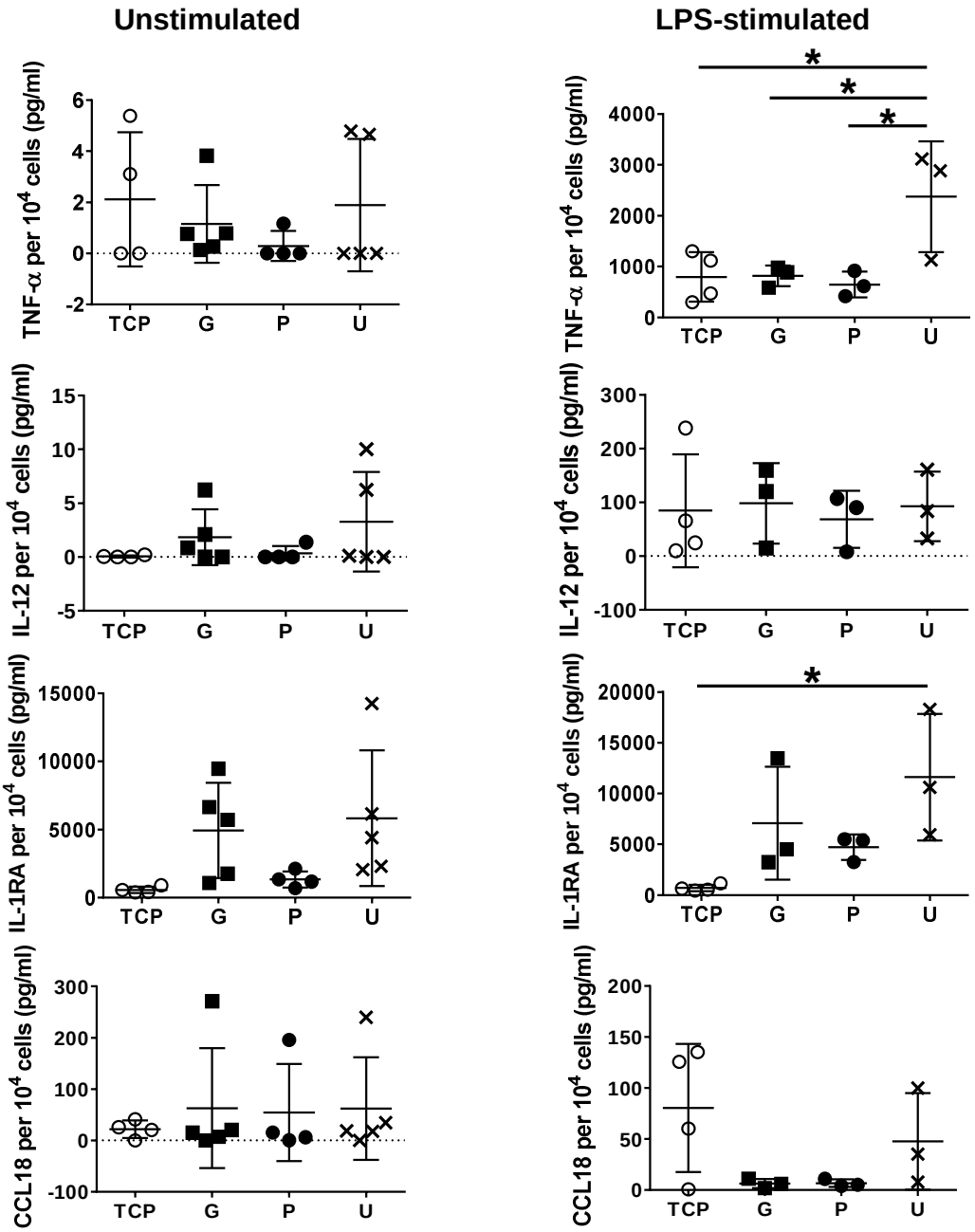

Figure 2. Cytokine production by macrophages on micropatterned GelMA hydrogels. Pro-inflammatory and anti-inflammatory cytokines and chemokines by human macrophages cultured on TCP, tissue culture plastic

controls and GelMA micropatterns: G, microgrooves/ridges; P, micropillars; U, unpatterned for 3 days (unstimulated) and after stimulation with 200 ng/ml LPS for 24 h (LPS-stimulated). Data presented are mean ± SD for at least n=3 donors. Significance was determined by one-way ANOVA with Tukey's post hoc test, * $p \leq 0.05$.

In order to study functional responses of macrophages cultured on micropatterned GelMA hydrogels, a phagocytosis assay was carried out using zymosan particles (Figure 3A). No significant differences were observed in the percentage of cells that had taken up zymosan particles or in the phagocytic index of the cells, although a trend towards reduced phagocytic index was observed in the micropillar condition (Figure 3B). However, a significant difference was observed between the mean number of zymosan particles per positive cell cultured on microgrooves/ridges vs. those on micropillars (G=15.19 particles per cell vs. P=10.89 particles per cell, p=0.0128, Figure 3B).

A

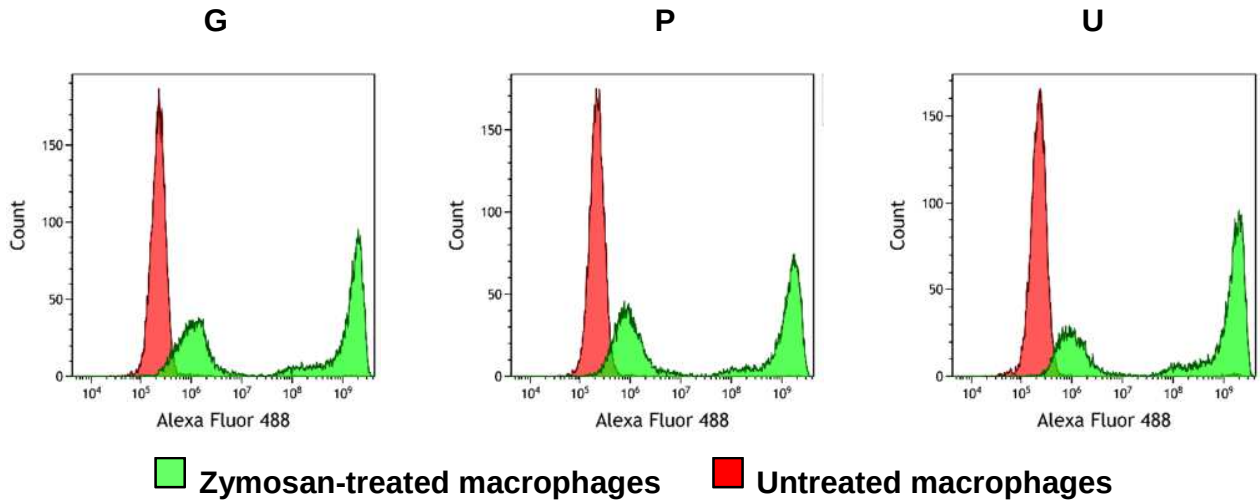

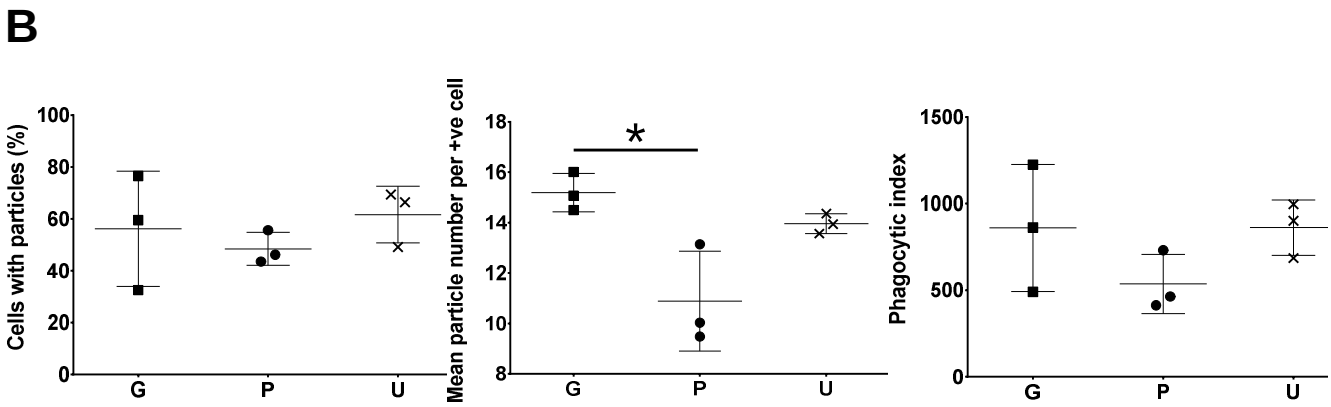

Figure 3. Phagocytosis by macrophages on micropatterned GelMA hydrogels. Phagocytosis of zymosan particles by human macrophages cultured on GelMA micropatterns: G, microgrooves/ridges; P, micropillars; U, unpatterned. Macrophages were treated with 10 particles/cell of zymosan at 37°C, 5% CO_2 for 30 min. **A.** Representative histograms of zymosan uptake by macrophages – red, untreated macrophages; green, zymosan-treated macrophages. **B.** Graphs depict the percentage of cells containing at least one zymosan particle (+ve cells), average number of particles per +ve cell, and phagocytic index. Data presented are mean ± SD for n=3 donors. Significance was determined by one-way ANOVA with Tukey's post hoc test, * $p \leq 0.05$.

Microarray analysis of macrophages cultured on patterned GelMA hydrogels

Gene microarray analysis was carried out in order to gain a global picture of topography-induced changes in macrophage gene expression. Using R, the relative expression data was processed for each individual array probe. An ANOVA and a pairwise Tukey's post-hoc test was conducted to identify conditions causing significant changes in gene expression.

Principal component analysis (PCA) and hierarchical clustering analysis of the significantly altered genes ($p<0.05$) showed that the different gel conditions – microgrooves/ridges, micropillars, and unpatterned – formed distinct clusters (Figure 4A), suggesting that this subset of genes can distinguish between macrophages cultured on different topographies. Hierarchical cluster analysis confirmed this (Figure 4B). 90 probes were identified to be significant in one or more pairwise comparison at $p<0.05$ (Figure S4 in Supporting Information), while 10 probes were significant at $p<0.01$ (Figure 5 and Table 2). Pairwise comparisons of the three hydrogel conditions suggested that micropillars had the greatest

impact on macrophage gene expression as the greatest number of significantly altered probes was observed for micropillars (Table S1 in Supporting Information).

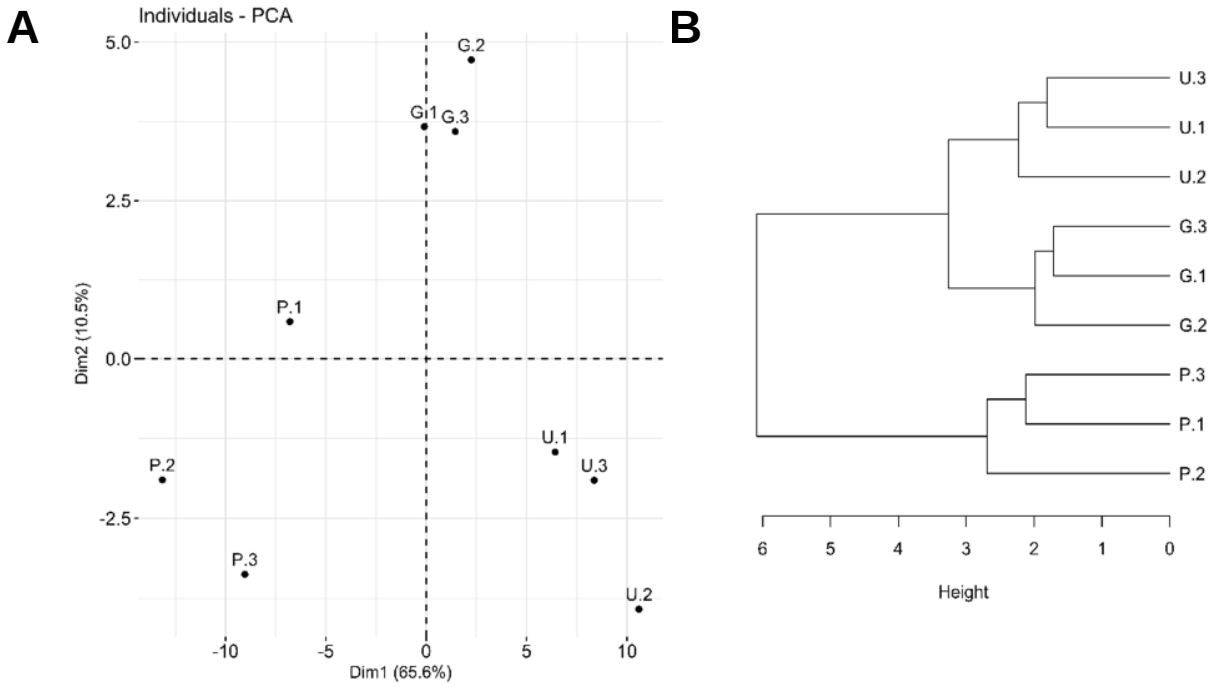

Figure 4. Principal component analysis (PCA) and cluster analysis of microarray data. A. PCA and **B.** cluster analyses of microarray data from 3 donors (1, 2 and 3 denote donors) were carried out in R. Only significantly altered genes ($p<0.05$ by one-way ANOVA with Tukey's post hoc test) were used to generate these plots. G, microgrooves/ridges; P, micropillars; U, unpatterned.

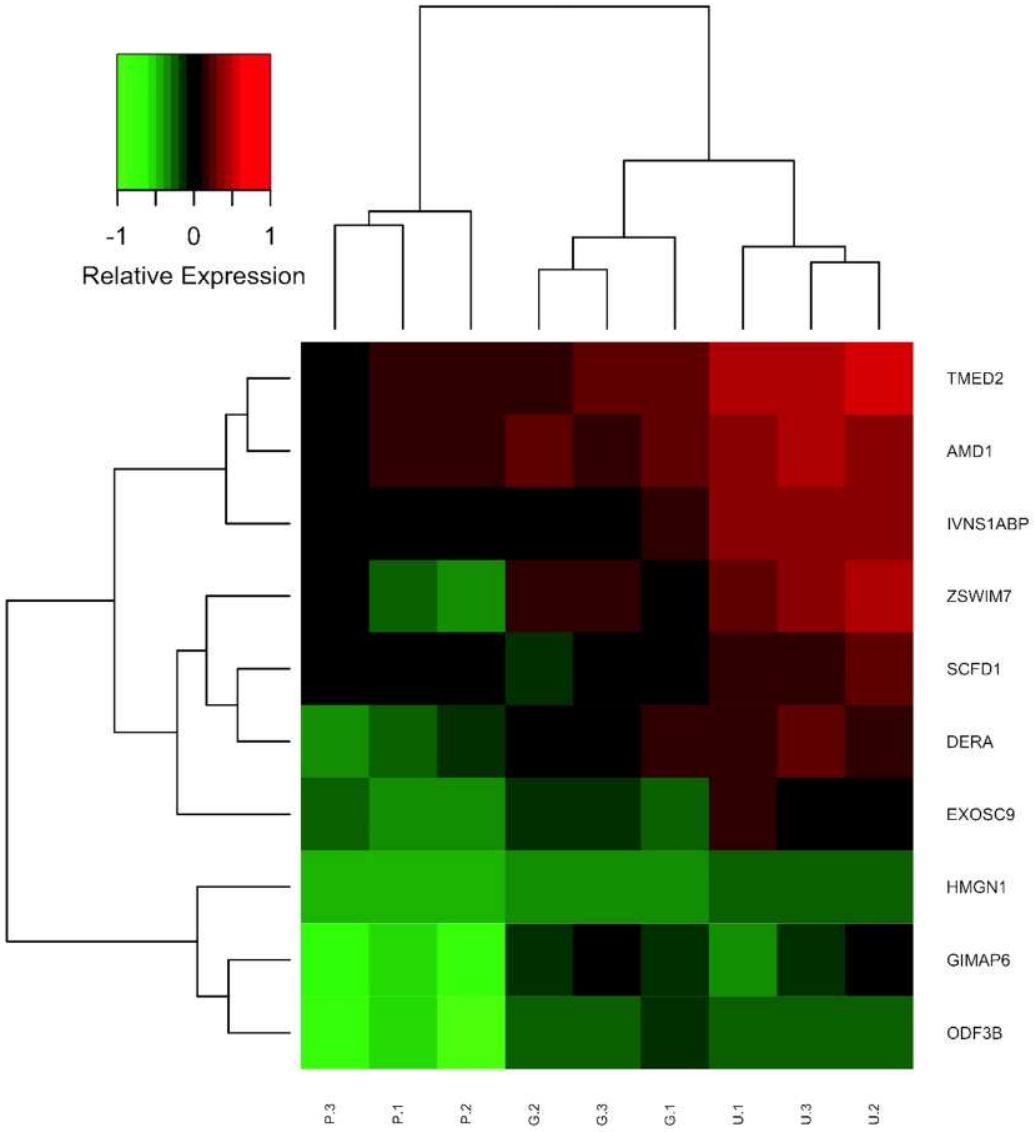

Figure 5. Heatmap of top 10 significantly altered genes from microarray data. Microarray results from 3 donors (1, 2 and 3 denote donors) were analysed in R. A heatmap of the top 10 significantly altered genes ($p<0.01$ by one-way ANOVA with Tukey's post hoc test) is presented here. G, microgrooves/ridges; P, micropillars; U, unpatterned.

Table 2: Relative expression of genes differentially expressed from microarray data.

Gene	Microgrooves/ridges (G)	Micropillars (P)	Unpatterned (U)
TMED2	+ [a]	++	+++
AMD1	+	+	++
IVNS1ABP	0 [b]	0	++
ZSWIM7	- [c]	+	++
SCFD1	0	0/-	+
DERA	-	0/+	+
EXOSC9	--	-	0/+
HMGN1	--	--	-
GIMAP6	---	-	-
ODF3B	---	-	-

[a] +, up-regulation, [b] 0, no change, [c] -, down-regulation, of expression compared to their respective TCP controls. Greater number of + or – symbols implies greater up- or down-regulation, respectively.

Finally, the 89 unique genes corresponding to the 90 probes significantly differentially expressed were processed to identify enriched Kyoto Encyclopaedia of Genes and Genomes (KEGG) pathways and gene ontology (GO) terms using the R script "NIPA" (https://github.com/ADAC-UoN/NIPA). In the Biological Processes category, 31 terms were identified to be significantly enriched compared to all genes in genome ($p<0.05$ hypogeometric test conducted with GOStats[43]). The top 10 of these are shown in Figure 6.

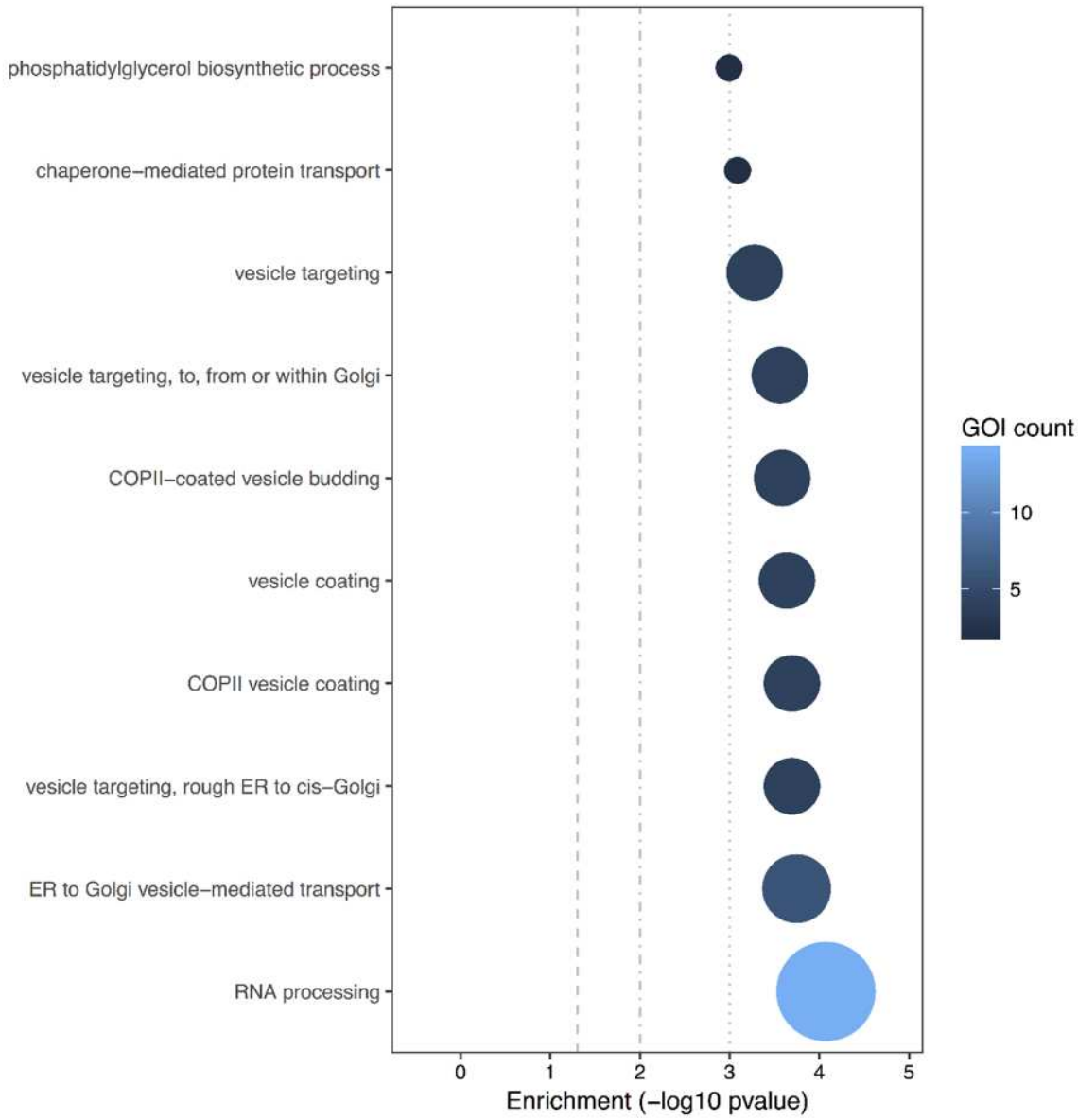

Figure 6. Gene ontology map of the top 10 biological processes that were significantly enriched compared to the rest of the genome. The size of the circle and colour represent the number of genes in each term within the differentially expressed gene list, X-axis represents enrichment –log10 p value.

DISCUSSION

This study presents novel data on the responses of human macrophages to micropatterned GelMA hydrogels. The rationale behind the study was to determine whether by modulating focal point adhesion and cell morphology using two specific microtopographies, namely micropillars and microgrooves/ridges, could modulate human macrophage phenotype, activation status and function. In order to assess macrophage behaviour we initially utilised conventional methods for determining macrophage phenotype (microscopy) and activation status (surface marker expression, cytokine secretion and phagocytosis) followed by an unbiased screening of global gene expression.

In our study, macrophage morphology was significantly different on GelMA hydrogels compared to TCP controls, with cells on TCP controls being larger, less elongated and having a greater cytoplasm to nucleus ratio. The vastly different chemistry and rigidity of TCP compared to GelMA could explain the significant difference in cellular morphology observed[27]. However, when comparing cell morphology on the different GelMA topographies (microgrooves/ridges vs. micropillars vs. unpatterned), despite observing transient changes, no significant difference was observed in any of the morphological descriptors. This is in contrast to studies with mouse macrophages that show significant changes in morphology on patterned surfaces such as greater elongation when constricted by 20 μm lines[32] or 3-5 μm wrinkles[31] compared to planar surfaces. One likely reason for differing observations in these studies compared to our study is that the materials used – PDMS[32], polyethylene films[31] and GelMA (present study) – have dissimilar chemical and stiffness profiles (e.g. mostly much stiffer than GelMA), which would result in differences in cell behaviour on these surfaces[27]. Another reason for discrepancies between the studies by McWhorter *et al.*[32] and Wang *et al.*[31] and the present study could be the differences between human and mouse macrophages. Human peripheral blood monocytes, and therefore, monocyte-derived macrophages, are a heterogeneous population[44] and as such will not respond to stimuli in a uniform way.

Surface topography has been used to induce changes in a number of cell types including immune cells such as macrophages[15]. For example, topography-induced elongation of mouse macrophages was shown to correspond to a more alternatively activated, anti-inflammatory phenotype in these cells[31-32]. However, a recent study by Malheiro *et al.* using the human monocytic cell line THP-1 (differentiated with phorbol 12-myristate 13-acetate, PMA, to resemble macrophages) showed no impact of topography on macrophage activation, although cell shape was altered[45]. Human macrophages can be differentially activated by topography, but the difference only seems to be apparent when comparing large-scale differences such as micropatterned vs. nanopatterned surfaces, as seen in a study by Paul *et al.* using human primary monocyte-derived macrophages on textured PVDF surfaces[36].

Nevertheless, the results of the present study indicate some changes in conventional measures of macrophage activation when using human macrophages and micropatterned surfaces. Patterning the GelMA hydrogels led to a significant decrease in production of the master pro-inflammatory cytokine TNF-α in response to LPS stimulation, although the type of pattern (microgrooves/ridges or micropillars) did not seem to be important in this process. LPS-stimulated macrophages on the patterned gels also appeared to produce less of the anti-inflammatory cytokine IL-1RA than those on unpatterned gels, but this was not significant. In addition, macrophages on the micropillars were found to phagocytose significantly less (~50%) zymosan particles than those on microgrooves/ridges and unpatterned gels. However, this did not correlate to a significant decrease in the phagocytic index of cells on micropillars. Finally, no significant difference was observed in the expression of MR (M2 marker) or calprotectin (M1 marker) or the percentage of the population expressing either of these markers on any of the topographies tested. Hence, these results indicate that micropatterned hydrogels can alter certain activation markers in human primary macrophages, although the observed profiles did not fit into strict M1 or M2 activation states, but probably represent a biomaterial-specific activation state.

In fact, this hypothesis is supported by the results of our gene microarray experiments, where the significantly different genes on the three hydrogel conditions (microgrooves/ridges, micropillars, and

unpatterned) were all related to primary metabolic processes. PCA using these significantly altered genes showed that the cells on each topography had a distinct gene expression profile, evidenced by the clear clustering of data points belonging to each group.

Ten probes were identified to show significantly different gene expression with different GelMA micropatterns (ANOVA with pairwise Tukey's post hoc test adjusted $p < 0.01$). These correspond to 10 genes: ODF3B, IVNS1ABP, DERA, GIMAP6, ZSWIM7, AMD1, HMGN1, EXOSC9, TMED2, SCFD1. These genes may be divided into different groups based on their cellular functions: 1) cell survival and proliferation, 2) protein trafficking and 3) regulation of nucleic acid processing and function.

The first group of genes, those playing a role in cell proliferation and survival, consists of four members – AMD1, GIMAP6, DERA, and IVNS1ABP. AMD1 (adenosylmethionine decarboxylase 1) encodes an intermediate enzyme in polyamine biosynthesis, essential for cellular proliferation and tumour promotion. GIMAP6 (GTPase, IMAP family member 6) encodes a member of the GTPases of immunity-associated proteins (GIMAP) family, which contain GTP-binding and coiled-coil motifs, and may play roles in the regulation of cell survival. DERA (Deoxyribose-Phosphate Aldolase) catalyses a reversible aldol reaction between acetaldehyde and D-glyceraldehyde 3-phosphate to generate 2-deoxy-D-ribose 5-phosphate. It participates in stress granule assembly and has been shown to permit cells in which mitochondrial ATP production was abolished to make use of extracellular deoxyinosine to maintain ATP levels[46]. IVNS1ABP (influenza virus NS1A binding protein) plays a role in cell division and in the dynamic organisation of the actin skeleton as a stabiliser of actin filaments by association with F-actin. It protects cells from cell death induced by actin destabilisation.

The second group of genes, those involved in protein trafficking, consists of two members – SCFD1 and TMED2. SCFD1 (sec1 family domain containing 1) plays a role in SNARE-pin assembly and Golgi-to-ER retrograde transport. TMED2 (transmembrane p24 trafficking protein 2) is involved in vesicular protein trafficking, acting in the early secretory pathway and post-Golgi membranes.

Finally, the third group of genes, which play a role in nucleic acid processing and function, consists of three members – ZSWIM7, HMGN1, and EXPSC9. ZSWIM7 (zinc finger SWIM-type containing 7) is involved in early stages of the homologous recombination repair pathway of double-stranded DNA breaks arising during DNA replication or induced by DNA-damaging agents. HMGN1 (high mobility group nucleosome binding domain 1) encodes a protein that binds nucleosomal DNA and is associated with transcriptionally active chromatin. Along with a similar protein, HMG17, it may help maintain an open chromatin configuration around transcribable genes. EXOSC9 (exosome component 9), transcript variant 2 (codes for isoform 2 of the protein) forms a component of the human exosome (an exoribonuclease complex which processes and degrades RNA in the nucleus and cytoplasm), binding to adenylate uridylate-rich element (ARE)-containing unstable RNAs. It may play a role in degradation and turnover of mRNA.

Thus, from the microarray results it would appear that GelMA hydrogel microtopographies may modulate cell survival and stress responses in macrophages. The data also indicate alterations in gene transcription, DNA repair, mRNA degradation, and protein trafficking by macrophages on micropatterened GelMA hydrogels. In general, micropatterning of GelMA appeared to down-regulate the expression of the top 10 significantly altered genes as compared to unpatterned GelMA. The down-regulation also appeared to be greater in the case of microgrooves/ridges than in the case of micropillars. The functional consequences of these changes in gene transcription need to be further investigated.

CONCLUSION

Our study supports the previous work[45] showing that microscale topographies on their own do not seem to significantly change macrophage polarization state based on the conventional readouts routinely used to assess macrophage activation status. Instead, our results indicate that changes in topography alter more fundamental processes in macrophages such as gene transcription, translation, protein trafficking, DNA repair and cell survival. This underlines the need for unbiased screening of macrophage responses

(especially human macrophages) in biomaterial and tissue engineering applications. These observations highlight the fact that when cells are exposed to conditions that are not highly polarising (e.g. surface topography), despite significant changes in the cells' key biological processes, conventional macrophage activation readouts may not indicate any changes and could even be misleading. Hence, in such cases, the use of very selective markers derived from cytokine-induced macrophage activation may lead to missed opportunities for fully understanding and exploiting macrophage-biomaterial interactions and the key cellular processes it can modulate. The adoption of an unbiased screening approach such as that demonstrated in the present study would have wide-reaching implications for understanding and modulating inflammation, foreign body responses and wound healing in response to biomaterials.

ACKNOWLEDGEMENTS

This project has received funding from the European Union's Seventh Framework Programme for research, technological development and demonstration under grant agreement no. 602694 (IMMODGEL).

SUPPORTING INFORMATION

Additional experimental details and results are shown in the supporting information document.

FUNDING SOURCES

EU FP7 grant no. 602694 (IMMODGEL)

REFERENCES

1. Gordon, S.; Pluddemann, A.; Martinez Estrada, F., Macrophage heterogeneity in tissues: phenotypic diversity and functions. *Immunological reviews* **2014,** *262* (1), 36-55.
2. Gosselin, D.; Link, V. M.; Romanoski, C. E.; Fonseca, G. J.; Eichenfield, D. Z.; Spann, N. J.; Stender, J. D.; Chun, H. B.; Garner, H.; Geissmann, F.; Glass, C. K., Environment drives selection and function of enhancers controlling tissue-specific macrophage identities. *Cell* **2014,** *159* (6), 1327-40.
3. Martinez, F. O.; Gordon, S., The M1 and M2 paradigm of macrophage activation: time for reassessment. *F1000prime reports* **2014,** *6*, 13.
4. Rostam, H. M.; Singh, S.; Salazar, F.; Magennis, P.; Hook, A.; Singh, T.; Vrana, N. E.; Alexander, M. R.; Ghaemmaghami, A. M., The impact of surface chemistry modification on macrophage polarisation. *Immunobiology* **2016,** *221* (11), 1237-46.
5. Mantovani, A.; Sica, A.; Sozzani, S.; Allavena, P.; Vecchi, A.; Locati, M., The chemokine system in diverse forms of macrophage activation and polarization. *Trends Immunol* **2004,** *25* (12), 677-86.
6. Hofkens, W.; Storm, G.; van den Berg, W.; van Lent, P., Inhibition of M1 macrophage activation in favour of M2 differentiation by liposomal targeting of glucocorticoids to the synovial lining during experimental arthritis. *Annals of the Rheumatic Diseases* **2011,** *70* (Suppl 2), A40.
7. Hao, N. B.; Lu, M. H.; Fan, Y. H.; Cao, Y. L.; Zhang, Z. R.; Yang, S. M., Macrophages in tumor microenvironments and the progression of tumors. *Clin Dev Immunol* **2012,** *2012*, 948098.
8. Hitesh Agrawal, S. S. T., Anthony E. Capito, David B. Drake, Adam J. Katz, Macrophage phenotypes correspond with remodeling outcomes of various acellular dermal matrices. *Open Journal of Regenerative Medicine* **2012,** *1* (3), 51-59.
9. Willenborg, S.; Lucas, T.; van Loo, G.; Knipper, J. A.; Krieg, T.; Haase, I.; Brachvogel, B.; Hammerschmidt, M.; Nagy, A.; Ferrara, N.; Pasparakis, M.; Eming, S. A., CCR2 recruits an inflammatory macrophage subpopulation critical for angiogenesis in tissue repair. *Blood* **2012,** *120* (3), 613-25.
10. Bartneck, M.; Schulte, V. A.; Paul, N. E.; Diez, M.; Lensen, M. C.; Zwadlo-Klarwasser, G., Induction of specific macrophage subtypes by defined micro-patterned structures. *Acta Biomater* **2010,** *6* (10), 3864-72.
11. Edin, S.; Wikberg, M. L.; Dahlin, A. M.; Rutegard, J.; Oberg, A.; Oldenborg, P. A.; Palmqvist, R., The distribution of macrophages with a M1 or M2 phenotype in relation to prognosis and the molecular characteristics of colorectal cancer. *PloS one* **2012,** *7* (10), e47045.
12. Mantovani, A., Macrophage diversity and polarization: in vivo veritas. *Blood* **2006,** *108* (2), 408-409.
13. Baitsch, D.; Bock, H. H.; Engel, T.; Telgmann, R.; Muller-Tidow, C.; Varga, G.; Bot, M.; Herz, J.; Robenek, H.; von Eckardstein, A.; Nofer, J. R., Apolipoprotein E induces antiinflammatory phenotype in macrophages. *Arterioscler Thromb Vasc Biol* **2011,** *31* (5), 1160-8.
14. Choi, K. M.; Kashyap, P. C.; Dutta, N.; Stoltz, G. J.; Ordog, T.; Shea Donohue, T.; Bauer, A. J.; Linden, D. R.; Szurszewski, J. H.; Gibbons, S. J.; Farrugia, G., CD206-positive M2 macrophages that express heme oxygenase-1 protect against diabetic gastroparesis in mice. *Gastroenterology* **2010,** *138* (7), 2399-409, 2409 e1.
15. Rostam, H. M.; Singh, S.; Vrana, N. E.; Alexander, M. R.; Ghaemmaghami, A. M., Impact of surface chemistry and topography on the function of antigen presenting cells. *Biomaterials science* **2015,** *3* (3), 424-41.
16. Patel, N. R.; Bole, M.; Chen, C.; Hardin, C. C.; Kho, A. T.; Mih, J.; Deng, L.; Butler, J.; Tschumperlin, D.; Fredberg, J. J.; Krishnan, R.; Koziel, H., Cell elasticity determines macrophage function. *PloS one* **2012,** *7* (9), e41024.
17. Blakney, A. K.; Swartzlander, M. D.; Bryant, S. J., The effects of substrate stiffness on the in vitro activation of macrophages and in vivo host response to poly(ethylene glycol)-based hydrogels. *Journal of biomedical materials research. Part A* **2012,** *100* (6), 1375-86.
18. Ahmed, E. M., Hydrogel: Preparation, characterization, and applications: A review. *Journal of Advanced Research* **2015,** *6* (2), 105-121.

19. Klotz, B. J.; Gawlitta, D.; Rosenberg, A. J. W. P.; Malda, J.; Melchels, F. P. W., Gelatin-Methacryloyl Hydrogels: Towards Biofabrication-Based Tissue Repair. *Trends in Biotechnology*.
20. Vegas, A. J.; Veiseh, O.; Doloff, J. C.; Ma, M.; Tam, H. H.; Bratlie, K.; Li, J.; Bader, A. R.; Langan, E.; Olejnik, K.; Fenton, P.; Kang, J. W.; Hollister-Locke, J.; Bochenek, M. A.; Chiu, A.; Siebert, S.; Tang, K.; Jhunjhunwala, S.; Aresta-Dasilva, S.; Dholakia, N.; Thakrar, R.; Vietti, T.; Chen, M.; Cohen, J.; Siniakowicz, K.; Qi, M.; McGarrigle, J.; Lyle, S.; Harlan, D. M.; Greiner, D. L.; Oberholzer, J.; Weir, G. C.; Langer, R.; Anderson, D. G., Combinatorial hydrogel library enables identification of materials that mitigate the foreign body response in primates. *Nature biotechnology* **2016,** *34* (3), 345-52.
21. Rivet, C. J.; Zhou, K.; Gilbert, R. J.; Finkelstein, D. I.; Forsythe, J. S., Cell infiltration into a 3D electrospun fiber and hydrogel hybrid scaffold implanted in the brain. *Biomatter* **2015,** *5*, e1005527.
22. Yu, T.; Wang, W.; Nassiri, S.; Kwan, T.; Dang, C.; Liu, W.; Spiller, K. L., Temporal and spatial distribution of macrophage phenotype markers in the foreign body response to glutaraldehyde-crosslinked gelatin hydrogels. *Journal of biomaterials science. Polymer edition* **2016**, 1-22.
23. Swartzlander, M. D.; Barnes, C. A.; Blakney, A. K.; Kaar, J. L.; Kyriakides, T. R.; Bryant, S. J., Linking the foreign body response and protein adsorption to PEG-based hydrogels using proteomics. *Biomaterials* **2015,** *41*, 26-36.
24. Yue, K.; Trujillo-de Santiago, G.; Alvarez, M. M.; Tamayol, A.; Annabi, N.; Khademhosseini, A., Synthesis, properties, and biomedical applications of gelatin methacryloyl (GelMA) hydrogels. *Biomaterials* **2015,** *73*, 254-71.
25. Nichol, J. W.; Koshy, S. T.; Bae, H.; Hwang, C. M.; Yamanlar, S.; Khademhosseini, A., Cell-laden microengineered gelatin methacrylate hydrogels. *Biomaterials* **2010,** *31* (21), 5536-44.
26. Aubin, H.; Nichol, J. W.; Hutson, C. B.; Bae, H.; Sieminski, A. L.; Cropek, D. M.; Akhyari, P.; Khademhosseini, A., Directed 3D cell alignment and elongation in microengineered hydrogels. *Biomaterials* **2010,** *31* (27), 6941-6951.
27. Teo, B. K.; Wong, S. T.; Lim, C. K.; Kung, T. Y.; Yap, C. H.; Ramagopal, Y.; Romer, L. H.; Yim, E. K., Nanotopography modulates mechanotransduction of stem cells and induces differentiation through focal adhesion kinase. *ACS Nano* **2013,** *7* (6), 4785-98.
28. McMurray, R. J.; Wann, A. K.; Thompson, C. L.; Connelly, J. T.; Knight, M. M., Surface topography regulates wnt signaling through control of primary cilia structure in mesenchymal stem cells. *Sci Rep* **2013,** *3*, 3545.
29. Pagliara, S.; Franze, K.; McClain, C. R.; Wylde, G. W.; Fisher, C. L.; Franklin, R. J.; Kabla, A. J.; Keyser, U. F.; Chalut, K. J., Auxetic nuclei in embryonic stem cells exiting pluripotency. *Nat Mater* **2014,** *13* (6), 638-44.
30. McNamara, L. E.; Burchmore, R.; Riehle, M. O.; Herzyk, P.; Biggs, M. J.; Wilkinson, C. D.; Curtis, A. S.; Dalby, M. J., The role of microtopography in cellular mechanotransduction. *Biomaterials* **2012,** *33* (10), 2835-47.
31. Wang, T.; Luu, T. U.; Chen, A.; Khine, M.; Liu, W. F., Topographical modulation of macrophage phenotype by shrink-film multi-scale wrinkles. *Biomaterials science* **2016**.
32. McWhorter, F. Y.; Wang, T.; Nguyen, P.; Chung, T.; Liu, W. F., Modulation of macrophage phenotype by cell shape. *Proceedings of the National Academy of Sciences of the United States of America* **2013,** *110* (43), 17253-8.
33. Garg, K.; Pullen, N. A.; Oskeritzian, C. A.; Ryan, J. J.; Bowlin, G. L., Macrophage functional polarization (M1/M2) in response to varying fiber and pore dimensions of electrospun scaffolds. *Biomaterials* **2013,** *34* (18), 4439-51.
34. Bota, P. C.; Collie, A. M.; Puolakkainen, P.; Vernon, R. B.; Sage, E. H.; Ratner, B. D.; Stayton, P. S., Biomaterial topography alters healing in vivo and monocyte/macrophage activation in vitro. *Journal of biomedical materials research. Part A* **2010,** *95* (2), 649-57.
35. Ma, Q. L.; Zhao, L. Z.; Liu, R. R.; Jin, B. Q.; Song, W.; Wang, Y.; Zhang, Y. S.; Chen, L. H.; Zhang, Y. M., Improved implant osseointegration of a nanostructured titanium surface via mediation of macrophage polarization. *Biomaterials* **2014,** *35* (37), 9853-67.
36. Paul, N. E.; Skazik, C.; Harwardt, M.; Bartneck, M.; Denecke, B.; Klee, D.; Salber, J.; Zwadlo-Klarwasser, G., Topographical control of human macrophages by a regularly microstructured polyvinylidene fluoride surface. *Biomaterials* **2008,** *29* (30), 4056-64.

37. Hwang, C. M.; Sim, W. Y.; Lee, S. H.; Foudeh, A. M.; Bae, H.; Lee, S. H.; Khademhosseini, A., Benchtop fabrication of PDMS microstructures by an unconventional photolithographic method. *Biofabrication* **2010,** *2* (4), 045001.
38. Nikkhah, M.; Eshak, N.; Zorlutuna, P.; Annabi, N.; Castello, M.; Kim, K.; Dolatshahi-Pirouz, A.; Edalat, F.; Bae, H.; Yang, Y.; Khademhosseini, A., Directed endothelial cell morphogenesis in micropatterned gelatin methacrylate hydrogels. *Biomaterials* **2012,** *33* (35), 9009-18.
39. Du, Y.; Lo, E.; Vidula, M. K.; Khabiry, M.; Khademhosseini, A., Method of Bottom-Up Directed Assembly of Cell-Laden Microgels. *Cellular and molecular bioengineering* **2008,** *1* (2), 157-162.
40. Selimovic, S.; Oh, J.; Bae, H.; Dokmeci, M.; Khademhosseini, A., Microscale Strategies for Generating Cell-Encapsulating Hydrogels. *Polymers* **2012,** *4* (3), 1554.
41. Garcia-Nieto, S.; Johal, R. K.; Shakesheff, K. M.; Emara, M.; Royer, P. J.; Chau, D. Y.; Shakib, F.; Ghaemmaghami, A. M., Laminin and fibronectin treatment leads to generation of dendritic cells with superior endocytic capacity. *PloS one* **2010,** *5* (4), e10123.
42. Carpenter, A. E.; Jones, T. R.; Lamprecht, M. R.; Clarke, C.; Kang, I. H.; Friman, O.; Guertin, D. A.; Chang, J. H.; Lindquist, R. A.; Moffat, J.; Golland, P.; Sabatini, D. M., CellProfiler: image analysis software for identifying and quantifying cell phenotypes. *Genome Biol* **2006,** *7* (10), R100.
43. Falcon, S.; Gentleman, R., Using GOstats to test gene lists for GO term association. *Bioinformatics* **2007,** *23* (2), 257-8.
44. Grubczak K., M. M., The role of different monocyte subsets and macrophages in asthma pathogenesis. *Prog Health Sci* **2015,** *5* (1), 176-184.
45. Malheiro, V.; Lehner, F.; Dinca, V.; Hoffmann, P.; Maniura-Weber, K., Convex and concave micro-structured silicone controls the shape, but not the polarization state of human macrophages. *Biomaterials science* **2016,** *4* (11), 1562-1573.
46. Salleron, L.; Magistrelli, G.; Mary, C.; Fischer, N.; Bairoch, A.; Lane, L., DERA is the human deoxyribose phosphate aldolase and is involved in stress response. *Biochim Biophys Acta* **2014,** *1843* (12), 2913-25.

"For Table of Contents Use Only"

Unbiased Analysis of the Impact of Micropatterned Biomaterials on Macrophage Behaviour Provides Insights beyond Pre-defined Polarisation States

Sonali Singh, Dennis Awuah, Hassan M. Rostam, Richard D. Emes, Navrohit K. Kandola, David Onion, Su Htwe, Buddharaksa Rajchagool, Byung-Hyun Cha, Duckjin Kim, Patrick J. Tighe, Nihal E. Vrana, Ali Khademhosseini, Amir Ghaemmaghami